Probabilistic Analysis of Wake Vortex Hazards for Landing Aircraft Using Multilateration Data

John F. Shortle*
Systems Engineering and Operations Research
George Mason University
4400 University Dr., MS 4A6
Fairfax, VA 22030
Tel: 703-993-3571
Fax: 703-993-1521
e-mail: jshortle@gmu.edu

Babak G. Jeddi
Systems Engineering and Operations Research
George Mason University
4400 University Dr., MS 4A6
Fairfax, VA 22030
Tel: 703-993-1623
Fax: 703-993-1521
e-mail: bghalebs@gmu.edu

* Corresponding author

Word Count: 4,876
Number of Figures: 10
Submission Date: 11/15/06

ABSTRACT

Wake vortices are a safety hazard to landing aircraft. A landing aircraft that encounters a wake may roll, resulting in a fatal crash if the roll is severe enough and/or if the aircraft is low enough to the ground. Therefore, aircraft are separated by a sufficient distance to ensure that wakes have time to decay in strength. However, because of the inherent variability in wake behavior and aircraft separation and position, there is still a possibility for a wake encounter. The objective of this paper is to estimate the probability of such encounters. This paper presents a hybrid simulation methodology. The approach is hybrid in the sense that part of the simulation is conducted using a direct data feed of flight-track data, while the other part is obtained by simulation of wake-evolution models. We demonstrate the approach on a one-week sample of flight tracks to predict the frequency of potential wake alerts. In this paper a wake alert is defined to be an event where the trailing aircraft is in a *region* of space where the wake is likely to be. We show how the results depend on atmospheric conditions and other model parameters.

INTRODUCTION

The objective of this paper is to present a methodology for simulating the probability of a wake vortex encounter, using flight-track records. Wake vortices are produced by airplanes as they fly (Figure 1). The vortices are coherent rotating flows of air. A trailing aircraft that flies through a wake may experience an upward force on one wing and a downward force on the other, producing a roll. If the encounter is severe enough, and/or if the aircraft is low enough to the ground, this can lead to a fatal crash.

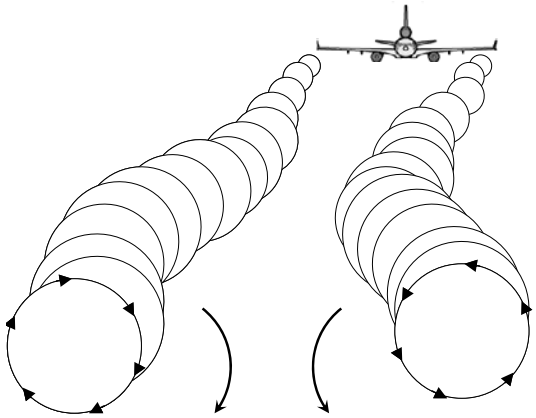

FIGURE 1 Wake vortices from an airplane.

Because of this potential hazard, aircraft must be separated by a distance to ensure that wakes decay to a sufficiently low strength (see reference (*1*) for a history of the separation standards). For example, the required separation during Instrument Flight Rules (IFR) between two landing aircraft at the runway threshold is between 2.5 and 6 nautical miles (nm), where the distance is a function of the weight categories of each plane (heavy, B757, large, and small).

Separation requirements are one of the key bottlenecks in the capacity of airports. This is particularly true for airports with closely spaced parallel runways, where adverse weather can reduce two runways to an effective capacity of one runway. The Federal Aviation Administration (FAA) and the National Aeronautics and Space Administration (NASA) are currently investigating changes to the wake separation rules for closely spaced parallel runways (*2*). Of course, before changes can be made, they must be demonstrated to be safe.

A challenge to ensuring safety is the inherent variability in wake behavior and the inherent variability in aircraft separation and position. By simulating both sources of variance – that is, by simulating stochastic aircraft trajectories and by also simulating the evolution of their wakes, it is possible to estimate the probability of a wake encounter. This basic approach has been taken by several researchers – for example (*3*, *4*). In this paper, we take a hybrid approach, where the variability in aircraft position is obtained using input flight-track data, rather than using simulation. Wake positions are obtained using simulation of wake-evolution models. Such a hybrid model could potentially be integrated with a live radar track feed and used as a real-time wake safety monitor.

This paper is organized as follows. First, we discuss the overall hybrid simulation approach. We describe the method for obtaining flight tracks from multilateration data and the method for implementing wake evolution models. Then, we present sample results based on one week of multilateration data. Sensitivity analysis is performed on various atmospheric parameters. Finally, we discuss conclusions and limitations in the work.

APPROACH

A wake vortex encounter occurs when a trailing aircraft flies through the vortex of a leading aircraft. Thus, two key pieces of information are needed to predict a wake encounter – the position of the trailing aircraft and the position and strength of the wake from the leading aircraft. Other factors may also be considered such as encounter geometry, encounter duration, size of the trailing aircraft, control authority of the trailing aircraft, pilot response, and so forth. In this paper, we only consider the position of the trailing aircraft, and the position and strength of the wake vortex in determining a potential hazard from a wake (Figure 2).

In general, it is much easier to model and predict the location of an airplane, compared to the location of a wake. An airplane can be tracked using radar or other surveillance methods. A wake is invisible. To track a wake,

one must measure and identify coherent patterns of rotating air. These patterns must be distinguished from similar patterns occurring naturally in the atmosphere. Thus, it can be difficult sometimes to distinguish between a "wake" and a "non-wake."

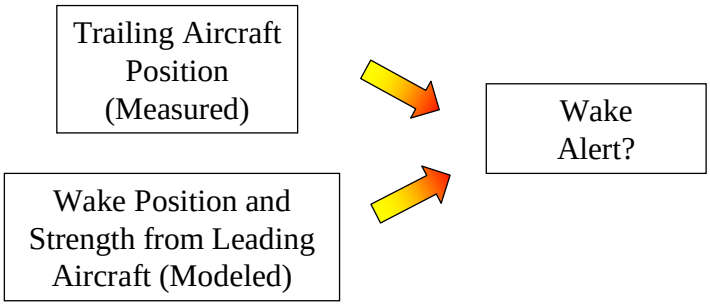

FIGURE 2 Elements of simulation approach.

In this paper, we model the locations of aircraft using flight tracks obtained from multilateration data. Conversely, we obtain the locations of wakes using simulation of wake-evolution models. The combined simulation is partly data-based and partly model-based.

Figure 3 shows the approach path for aircraft landing at a single runway. The leading and trailing aircraft follow the same approximate path along the glideslope and localizer. The wake from the leading aircraft decays in strength over time and typically sinks vertically. At any point x along the approach path, the trailing aircraft may encounter the wake from the leading aircraft. More specifically, when the trailing aircraft is at longitudinal position x, a wake encounter occurs if *all* three of the following events occur simultaneously:

- The lateral positions of the trailing aircraft and the wake (at longitudinal position x) overlap,
- The vertical positions of the trailing aircraft and the wake (at longitudinal position x) overlap, *and*
- The circulation of the wake (at longitudinal position x) has not decayed below a specified threshold.

In summary, a wake encounter involves three dimensions – lateral, vertical, and time. Separation must be lost in all three dimensions for a wake encounter to occur. Said another way, if separation is maintained in at least one dimension, a wake encounter is prevented. (The time dimension is like the longitudinal dimension. If two aircraft are separated in the longitudinal dimension – say, by 3 nm – then, they are likely to have a sufficient separation in time.)

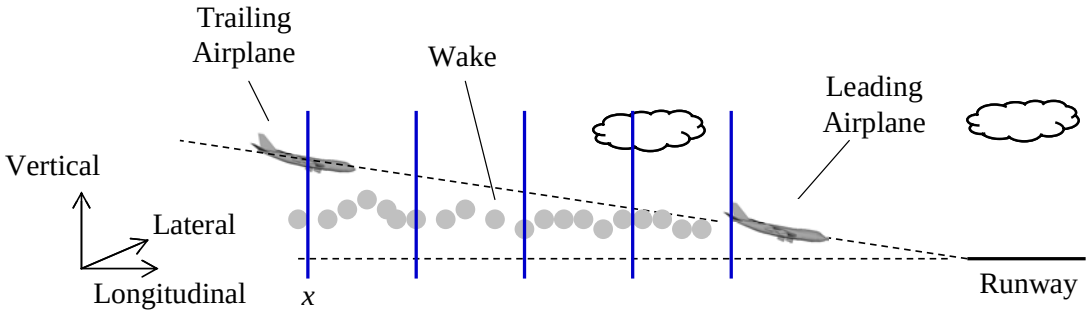

FIGURE 3 Wake hazard along the approach path.

In this paper, instead of predicting a wake *encounter*, we predict an event which we call a wake *alert*. A wake alert is defined to be an event where the trailing aircraft enters a *region* of space where the wake is *likely* to be (versus passing through a specific point). We take this approach, because there are inherent limitations in predicting the location of a wake vortex, due to inherent variability in atmospheric conditions and the sensitivity of wake behavior to these conditions. More specifically, we define a wake alert and the region of space where the wake is likely to be as follows: A wake alert occurs when the trailing aircraft is at longitudinal position x (see Figure 3) and the following events occur simultaneously:

- The vertical position of the trailing aircraft is *below* the predicted vertical position of the wake (at longitudinal position x), *and*
- The circulation of the wake (at longitudinal position x) has not decayed below a specified threshold L.

This definition of a wake alert differs from the definition of a wake encounter in the following ways: (1) The lateral dimension is ignored. In other words, we assume a worst-case scenario in this dimension, where the lateral positions of airplanes and wakes coincide. (2) In the vertical dimension, we assume a potential wake danger whenever the trailing aircraft is *below* the predicted location of the wake. (3) The definition in the time dimension is the same. As a default, we use a wake threshold of $L = 70$ m^2/s, which is approximately the circulation strength of background air turbulence. This is a conservative threshold, since any wake slightly above the background turbulence counts as a potential wake hazard. In summary, a wake alert is a less severe event than a wake encounter, but it is a more likely event. The probability of a wake alert gives a conservative estimate (or upper bound) for the probability of a wake encounter.

FLIGHT TRACK DATA

A critical variable in predicting wake encounters is the time-separation of aircraft as they land. The probabilistic variation in time separation has been measured by various researchers. For example, (*5*) and (*6*) took direct, visual measurements of aircraft time-separations using binoculars and a stopwatch. (*7*) used the Performance Data Analysis and Reporting System database. (*8*) measured aircraft separations from radar data. Others have used multilateration data (*9*) and (*10*). In this paper, to demonstrate concepts, we use multilateration data collected at Detroit Metropolitan Wayne County Airport (DTW) over a one-week period. The data were collected and pre-processed by Sensis Corporation and the Volpe National Transportation Systems Center. Further processing and analysis were done in (*10*) to extract individual landing tracks and to obtain probability distribution fits to the data.

Figure 4 shows a sample plot of three flight tracks, looking down from above. The rectangle on the left is runway 21L. The coordinates have been rotated so that the runway is aligned with the *x*-axis. The *y*-axis is magnified, distorting the lateral variation of the aircraft tracks. At far distances from the runway threshold, the large variability in the tracks is likely due to increased inaccuracy in the multilateration data. From the figure, one can also see some of the taxi-way exits.

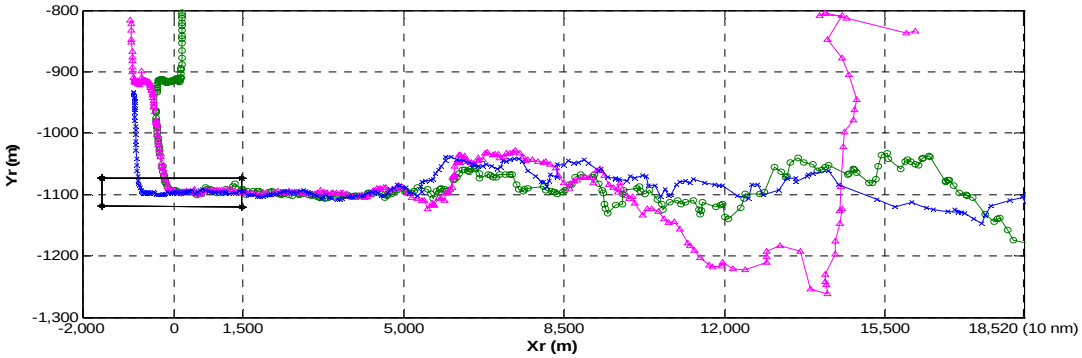

FIGURE 4 Three sample flight tracks.

Figure 5 shows the positions of aircraft at 6 nm, 5 nm, …, 0 nm from the runway threshold. This is one week of data (1190 distinct landings) at one runway, landing in the same direction. Because the multilateration system is not always able to track aircraft at far distances, and because some of the tracks are outside the bounds of the plots at these distances, there are fewer recorded points at 6 nm than at 0 nm. The figure shows a clear pattern, consistent with expectations: The variability in position decreases as the aircraft get closer to the runway.

WAKE VORTEX MODELS

Wake vortices can be measured in several ways – for example, using light or sound. Some examples of wake measurements using light (specifically, using a LIDAR instrument – LIght Detection And Ranging) are given in (*11, 12*). An example of wake measurements using sound is given in (*13*).

The approach in this paper is to use models of wake behavior, since there are no wake measurements that correspond to the flight tracks at DTW. Numerous researchers have developed models to characterize wake behavior. An early model was given in (*14*). This model, along with modifications in (*15*), forms the basis for the NASA AVOSS Prediction Algorithm (APA) (*16*). Other examples include (*17*), the large eddy simulation Terminal Area Simulation System (TASS) (*18*), a fast-time derivative TDAWP (TASS Driven Algorithms for Wake Prediction) (*19*), and the Probabilistic Two-Phase wake model (P2P) (*20*).

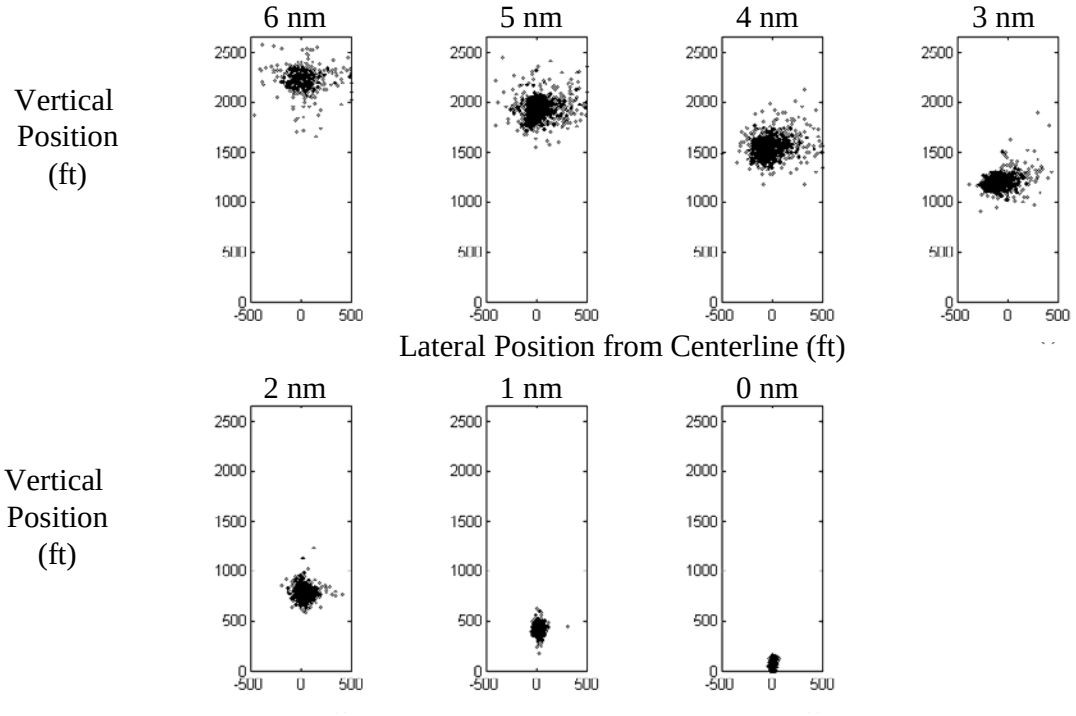

FIGURE 5 Cross-sectional plots of flight tracks at 1 nm intervals.

In this paper, we use the P2P model. The main reason is that it can be easily implemented in code, it is relatively fast to compute, and it provides probabilistic bounds for the locations of the wakes. Of course, there is nothing to prevent implementation of the other algorithms in the same context described in this paper. In particular, the fast-time simulation TDAWP (*19*) is similar in spirit to the P2P model. Both are based on fitting approximating differential equations to the output of large eddy simulation models. The resulting differential equations are fast to numerically integrate, compared with the large eddy simulation models.

The primary inputs to P2P are: aircraft velocity *V*, aircraft mass *M*, aircraft wing span *B*, air density ρ, eddy dissipation rate (EDR) ε, and Brunt-Vaisala frequency *N*. The initial behavior of the wake vortices is characterized by the following parameters (these constants and equations are typical of many wake models):

- The initial wake circulation is $\Gamma_0 = Mg/(\rho sBV)$, with units of m^2/s, where $s = \pi / 4$ is a constant.
- The initial lateral spacing of the vortices is $b_0 = sB$.
- The initial descent velocity is $w_0 = \Gamma_0/(2\pi b_0)$.
- The approximate time for the wakes to descend one initial vortex spacing is $t_0 = b_0 / w_0 = 2\pi b_0^2 / \Gamma_0$.

Frequently, the outputs of wake models are expressed in normalized units, where circulation is normalized by Γ_0, position is normalized by b_0, time is normalized by t_0, and velocity is normalized by $w_0 = b_0 / t_0$.

In P2P, the wake behavior further depends on two atmospheric parameters, ε and *N*. Eddy dissipation rate ε is a measure of turbulence in the atmosphere, where higher values correspond to greater turbulence. The Brunt-Vaisala frequency *N* is a measure of the vertical gradient of potential temperature in the atmosphere. The basic idea is that as a mass of air (for example, a wake) sinks, the surrounding air increases in density relative to the air mass. This causes an upward buoyancy force on the air mass, leading to a vertical oscillation. When $N = 0$ (per second), there is no buoyancy force and the air is said to be neutrally stratified. Higher values of *N* correspond to a greater buoyancy force. In particular, sinking wakes may "bounce" in such conditions. The normalized versions of these values are:

$$\varepsilon^* \equiv \frac{(\varepsilon b_0)^{1/3}}{w_0} = \frac{2\pi\varepsilon^{1/3} b_0^{4/3}}{\Gamma_0} \quad \text{and} \quad N^* \equiv N \cdot t_0 = N \cdot \frac{b_0}{w_0}. \tag{1}$$

Figure 6 shows a sample output of P2P. The input parameters for this figure are: aircraft velocity V = 80 m/s (about 155 knots), aircraft mass M = 273,000 kg (about 600,000 lbs), aircraft wing span B = 64.4 m (about 210 ft), air density ρ = 1.2 kg / m^3, ε = 0 m^2/s^3 (no turbulence), and N = 0 / sec. (neutral stratification). The corresponding reference values are initial circulation Γ_0 = 551 m^2/s, initial wake spacing b_0 = 50.6 m, initial descent velocity w_0 = 1.73 m/s, and reference time t_0 = 29.2 s.

The figure shows several core features of the P2P (Probabilistic Two-Phase) model. First, there are two phases of decay – a period of slower decay followed by a period of faster decay. Since wake descent is positively correlated with circulation strength, the period of faster decay corresponds to a period of reduced descent. A second key feature is the probabilistic component, expressed as upper and lower bounds to circulation and wake descent. The precise method for computing these bounds is described in (*20*). When the age of the wake is zero, these bounds correspond to +/- 0.20 Γ_0 for circulation strength and +/- b_0 for wake descent. The middle curve is a deterministic run of the P2P model, corresponding to a predicted average behavior.

In terms of the definition of a wake alert, we conservatively define a wake alert with respect to the upper bounds of circulation and height. That is, when the aircraft is below the upper bound of wake height, and when the upper bound of circulation strength is greater than the minimum threshold, we say a wake alert occurs.

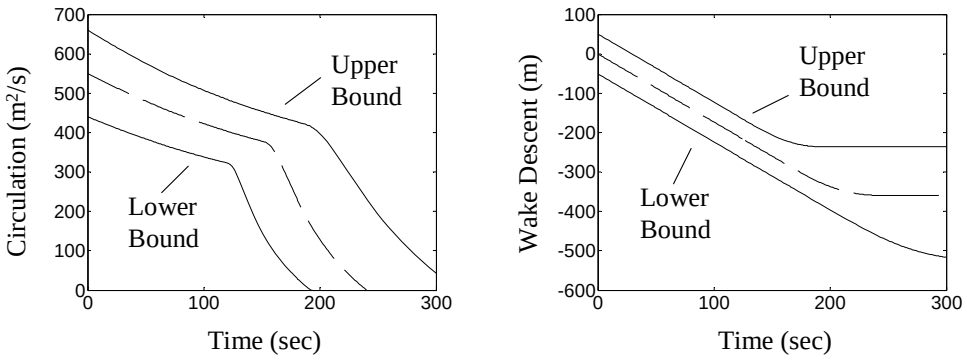

FIGURE 6 Sample output from P2P model.

Figure 7 shows sample effects of EDR ε and Brunt-Vaisala frequency N on wake circulation (see also figure 2 in (*20*)). To avoid clutter, the figure shows only the deterministic / middle prediction of P2P. The atmospheric parameters are expressed in normalized units ε^* and N^*, as in equation 1. The other inputs are as before: V = 80 m/s, M = 273,000 kg, B = 64.4 m, and ρ = 1.2 kg / m^3. The figure shows the following main effects. An increase in turbulence ε^* leads to a faster onset of the rapid decay phase. Similarly, an increase in stratification N^* leads to a faster onset of the rapid decay phase. The combined effect of increasing both variables is less than the sum of the individual effects.

RESULTS

In this section, we first show sample output from the simulation for a single pair of landings, and then give results over a range of landings. Figure 8 shows sample output for two consecutive landings. The upper right figure shows the vertical profile of the two aircraft trajectories (from a side view perspective). These trajectories are obtained from the multilateration data. Here, the higher curve corresponds to the leading aircraft and the lower curve corresponds to the trailing aircraft. In this example, the potential for a wake encounter is evaluated 3 nm from the threshold. This is denoted by the vertical line in the upper right graph. The location of the trailing aircraft at the 3 nm mark is identified by the star in the graph.

To obtain input parameters for the P2P model, the velocity of the lead aircraft is V = 71.3 m/s (138.7 kts), estimated from the multilateration data by taking the average velocity of the aircraft over the last 6 nm to the threshold. For the aircraft wingspan and mass, we use assumed values of B = 48.8 m (160 ft) and M = 67,120 kg (148,000 lbs). These values correspond to an aircraft on the higher end of the "large" weight category. Since 91% of the landings are large aircraft or smaller (*10*), these values represent conservative weight and wingspan estimates for most of the landings. The air density is assumed to be 1.2 kg/m^3 and the atmospheric parameters ε and N are assumed to be 0.

The two graphs on the left show the height and circulation strength of the wake from the lead aircraft at 3 nm from the threshold. Both graphs have an upper bound, a lower bound, and a mid-range estimate, as computed by the P2P model. The graphs show the wake evolution as a function of time. Time $t = 0$ corresponds to the moment when the lead aircraft passes the 3 nm mark. In particular, at $t = 0$ the wake height (specifically, the mid-range height, dashed line) is the same as the height of the leading aircraft at the 3 nm mark, which can be seen in the graph to the right. The circulation strength at $t = 0$ is Γ_0, as computed in the previous section.

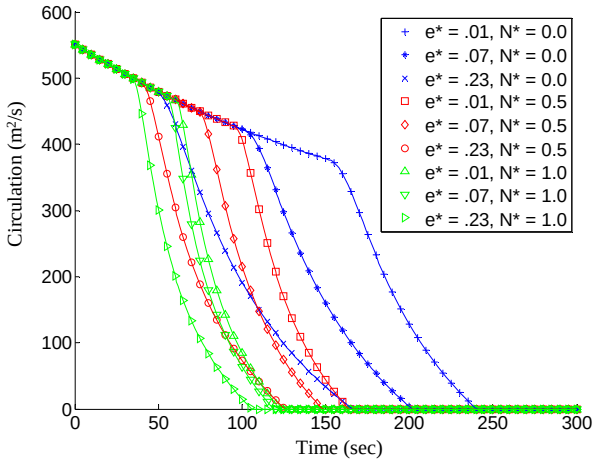

FIGURE 7 Effects of atmospheric parameters on wake decay (based on P2P model).

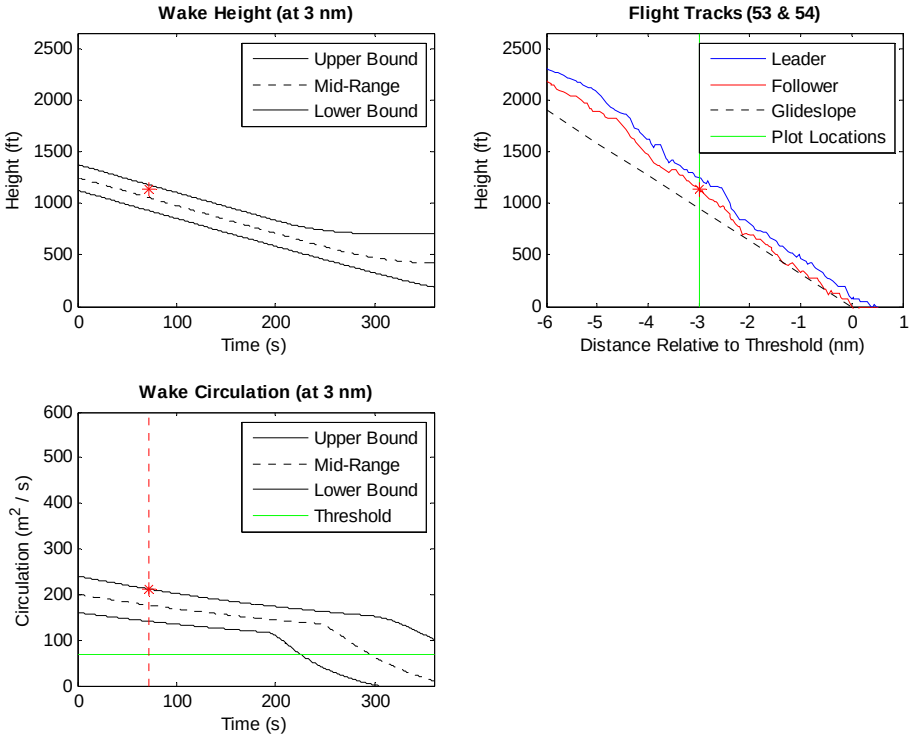

FIGURE 8 Simulation output for one pair of landings.

Now, for this particular pair of aircraft, the time separation (at the 3 nm mark) between the leading aircraft and the trailing aircraft is 72 seconds, obtained from multilateration data. The star in the upper left figure corresponds to the trailing aircraft as it passes the 3 nm mark. The *x*-value of this point is the time separation of the two aircraft. In other words, when the trailing aircraft passes the 3 nm mark, the wake from the leading aircraft is 72

seconds old. The *y*-value for this point is the vertical height of the trailing aircraft at the 3 nm mark, which can also be seen in the upper right graph. In other words, the star shows the location of the trailing aircraft relative to the wake of the leading aircraft as it passes the 3 nm mark. Now, because the star lies below the P2P upper bound (though not the mid-range estimate), we have the potential for a wake alert. In this case, this is partially due to a short separation time (72 seconds) and that the leading aircraft takes a higher trajectory than the trailing aircraft.

On the lower left figure, the star denotes the upper bound of wake circulation at the time the trailing aircraft crosses the 3 nm mark. Again, the wake is 72 seconds old at this time, and the estimate for the upper bound of circulation strength is approximately 230 m^2/s. Because this value is greater than the assumed minimum threshold of 70 m^2/s, the condition for a wake alert is satisfied.

In summary, for this pair of aircraft, we have a wake alert at the 3 nm mark because (a) the trailing aircraft is below the upper bound of the predicted wake height at this point, and (b) the circulation strength of the wake at this time is above the minimum threshold (70 m^2/s). Both conditions must be met for a wake alert. In the simulation model, all parameters – for example, the atmospheric parameters ε and *N* and the minimum wake threshold 70 m^2/s – can be easily adjusted, and the analysis re-run.

This example illustrates the main logic for computing wake alerts from the multilateration data and wake model. We now apply this logic to a week of landings (1190 landings) at a single runway. Figure 9 shows sample results, based on varying the atmospheric parameters ε and *N*. The plotted function is the probability of a wake alert. Keep in mind, we have defined wake alerts very conservatively. A wake alert represents a heightened probability of a wake encounter – based on conservative assumptions – and does not necessarily imply a wake encounter.

In general, higher values of ε and *N* lead to a faster onset of the rapid decay phase. Thus, we expect that the probability of a wake alert decreases in ε and *N*. In the figure, this is observed for larger values of both ε and *N*. However, for small EDR ε, the wake alert probability increases in *N*. This is because increased stratification (higher *N*) causes the wake to sink less quickly and even to "bounce" back up. Thus, even though the wake decays more quickly, it is at a higher altitude, and does not decay quickly enough (below 70 m^2/s) to be out of the path of the trailing aircraft. A similar effect is observed when *N* is small and ε increases. Increasing ε causes a faster onset of the rapid decay phase. In turn, this causes the wake to sink more slowly. Even though the wake decays more quickly, it is at a higher altitude, and does not decay quickly enough (below 70 m^2/s), so it is in the path of the trailing aircraft.

This counter-intuitive effect is not as pronounced when we increase the wake threshold. Figure 10 shows the same analysis, but with a minimum wake threshold of 125 m^2/s. With this higher threshold, the wake alert probability is generally much smaller than in Figure 9. It also displays the expected pattern of decreasing as ε and *N* increase.

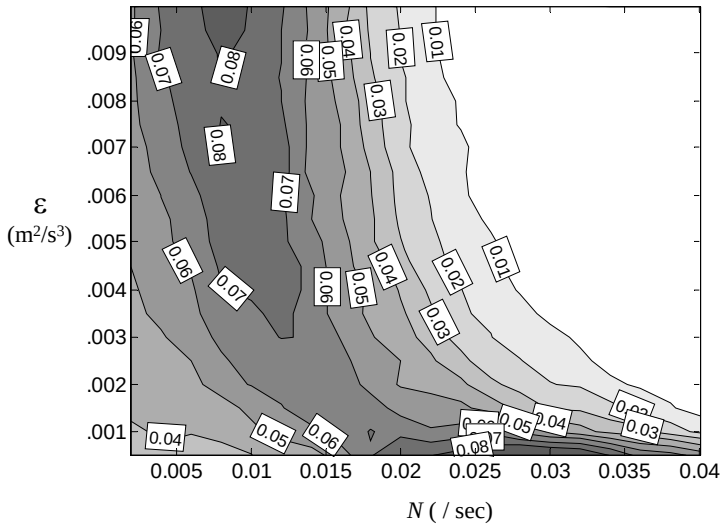

FIGURE 9 Sample wake alert probability, with wake threshold 70 m^2/s.

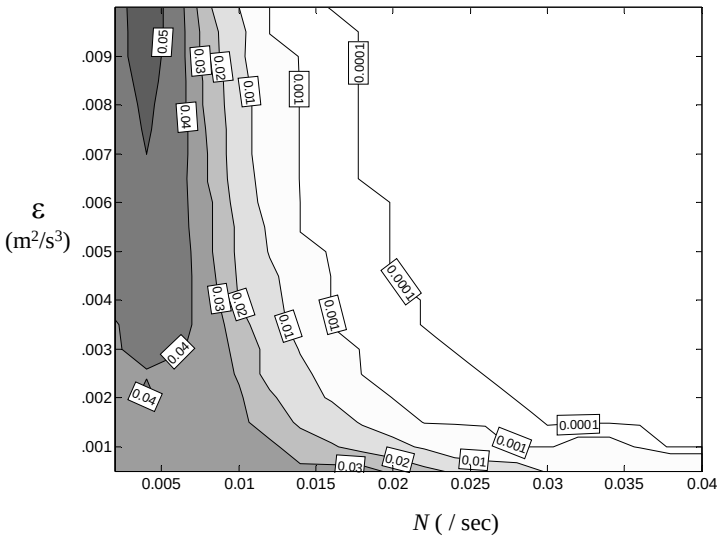

FIGURE 10 Sample wake alert probability, with wake threshold 125 m²/s.

CONCLUSIONS

Before discussing conclusions, we note several limitations and assumptions of this analysis. All results presented in this paper must be qualified with these assumptions.

- All aircraft are assumed to have the same wingspan and landing mass, representative of an aircraft on the high end of the "large" weight category. More accurate estimates could be obtained by linking the Mode-S identifier in the multilateration data to the specific type of aircraft.
- The vertical dimension of aircraft position is obtained through Mode-C pressure readings. The accuracy of the vertical dimension is less accurate than the lateral and longitudinal dimensions obtained from multilateration data. This is a critical variable.
- A wake encounter (or alert) is defined only with respect to wake circulation and not with respect to other variables, such as encounter duration, encounter geometry, pilot response, and so forth.
- Wakes are modeled using the P2P model. Some limitations of this model are:
  - It does not account for ground effects.
  - The percentage of wakes that are expected to fall within the probabilistic bounds is not defined.
- Furthermore, in our implementation of P2P, we make the following simplifications:
  - The lateral component of wake position is ignored.
  - Wind effects are ignored.
  - Single values for the atmospheric parameters ε and *N* are used at all altitudes.
  - The effect of root-mean-squared turbulence velocity on the *bounds* of descent height is omitted.

With these qualifying remarks, this paper has presented a methodology to estimate wake alert probabilities based on a direct feed of flight-track data. By varying atmospheric parameters in the accompanying wake models, one can see the potential range of probabilities over a variety of conditions. The analysis revealed a counter-intuitive effect: Even if the wakes decay more quickly, there is not necessarily a decrease in the wake-alert probability, because the wakes may remain for a longer period of time at a higher altitude before they decay in strength below the critical threshold. All of this highlights the importance of understanding the basic effects of environmental parameters on the wakes in multiple dimensions, also considering the stochastic behavior of airplane trajectories. Finally, such analysis has the potential to be extended and implemented in a real-time setting using a live feed of flight tracks to monitor the safety performance of arrival operations.

ACKNOWLEDGEMENTS

This paper solely represents the opinions of the authors and does not necessarily reflect the opinion of the United States government or NASA. The authors would like to thank Wayne Bryant and Ed Johnson at NASA Langley, for support of this research. We also thank the Volpe National Transportation Systems Center and Sensis Corporation for help in acquiring, manipulating, and understanding multilateration data.

REFERENCES

1. Burnham, D., and J. Hallock. Wake Vortex Separation Standards: Analysis Methods. Publication DOT/FAA/ND-97-4. FAA and U.S. Dept. of Transportation, 1997.
2. Lang, S., A. Mundra, W. Cooper, B. Levy, C. Lunsford, A. Smith, and J. Tittsworth. A Phased Approach to Increase Airport Capacity through Safe Reduction of Existing Wake Turbulence Constraints. *Air Traffic Control Quarterly*, Vol. 11, No. 4, 2003, pp. 331-356.
3. Speijker, L., G. van Baren, L. Sherry, J. Shortle, and F. Rico-Cusi. Assessment of Wake Vortex Separation Distances using the WAVIR Toolset. 23rd Digital Avionics Systems Conference, Salt Lake City, UT, 2004.
4. Kos, J., H. Blom, L. Speijker, M. Klompstra, and G. Bakker. Probabilistic Wake Vortex Induced Accident Risk Assessment. In *Air Transportation Systems Engineering*, G. Donohue and D. Zelwegger (eds.), AIAA, Lexington, MA, 2000, pp. 513-531.
5. Haynie, C. An Investigation of Capacity and Safety in Near-terminal Airspace Guiding Information Technology Adoption. Ph.D. Dissertation, George Mason University, Fairfax, VA, 2002.
6. Xie, Y. Quantitative Analysis of Airport Arrival Capacity and Arrival Safety using Stochastic Models. Ph.D. Dissertation, George Mason University, Fairfax, VA, 2005.
7. Rakas, J., and H. Yin. Statistical Modeling and Analysis of Landing Time Intervals: Case Study of Los Angeles International Airport, California. In *Transportation Research Record: Journal of the Transportation Research Board, No. 1915*, TRB, National Research Council, Washington, D.C., 2005, pp. 69-78.
8. Ballin, M., and H. Erzberger. An Analysis of Landing Rates and Separations at the Dallas / Fort Worth International Airport. NASA Technical Memorandum 110397, 1996.
9. Levy, B., J. Legge, and M. Romano. Opportunities for Improvements in Simple Models for Estimating Runway Capacity, 23rd Digital Avionics Systems Conference, Salt Lake City, UT, 2004.
10. Jeddi, B., J. Shortle, and L. Sherry. Statistics of the Approach Process at Detroit Metropolitan Wayne County Airport. In *Proceedings of the International Conference on Research in Air Transportation*, Belgrade, Serbia and Montenegro, 2006, pp. 85-92.
11. Dasey, T., S. Campbell, R. Heinrichs, M. Matthews, R. Freehart, G. Perras, and P. Salamitou. A Comprehensive System for Measuring Wake Vortex Behavior and Related Atmospheric Conditions at Memphis, Tennessee. *Air Traffic Control Quarterly*, Vol. 5, No. 1, 1997, pp. 49-68.
12. Chalson, M., J. Hallock, S. Mackey, M. Soares, F. Wang, D. Burnham, and S. Hannon. Data Supporting STL Proposed Change, WakeNet USA 2005, Boca Raton, FL, 2005.
13. Wang, F, H. Wassaf, and A. Gulsrud. Acoustic Imaging of Aircraft Wake Vortex Dynamics, 23rd AIAA Applied Aerodynamics Conference, Toronto, Ontario Canada, AIAA 2005-4849, 2005.
14. Greene, G. An Approximate Model of Vortex Decay in the Atmosphere. *Journal of Aircraft*, Vol. 23, No. 7, 1986, pp. 566-573.
15. Sarpkaya, T. New Model for Vortex Decay in the Atmosphere. *Journal of Aircraft*, Vol. 37, No. 1, 2000, pp. 53-61.
16. Robins, R., and D. Delisi. NWRA AVOSS Wake Vortex Prediction Algorithm Version 3.1.1. Publication NASA/CR-2002-211746, NASA, 2002.
17. Rossow, V., G. Hardy, and L. Meyn. Models of Wake-vortex Spreading Mechanisms and their Estimated Uncertainties. AIAA 5th Aviation, Technology, Integration, and Operations Conference (ATIO), Arlington, VA, 2005.
18. Switzer, G., and F. Proctor. Numerical Study of Wake Vortex Behavior in Turbulent Domains with Ambient Stratification. 38th Aerospace Sciences Meeting and Exhibit, Reno, NV, AIAA-2000-0755, 2000.
19. Proctor, F., D. Hamilton, and G. Switzer. TASS Driven Algorithms for Wake Prediction. 44th AIAA Aerospace Sciences Meeting and Exhibit, AIAA 2006-1073, Reno, NV, 2006.
20. Holzapfel, F. Probabilistic Two-phase Wake Vortex Decay and Transport Model. *Journal of Aircraft*, Vol. 40, No. 2, 2003, pp. 323-331.